HHS Public Access

Author manuscript

Nanomedicine. Author manuscript; available in PMC 2021 January 01.

Published in final edited form as:

Nanomedicine. 2020 January ; 23: 102090. doi:10.1016/j.nano.2019.102090.

Bioactive proteins delivery through core-shell nanofibers for meniscal tissue regeneration

Jihye Baek, PhD[a,b], **Emily Lee, BS**[a,b], **Martin K Lotz, MD**[b], **Darryl D D'Lima, MD, PhD**[a,b,*]

[a]Shiley Center for Orthopaedic Research and Education at Scripps Clinic, 10666 North Torrey Pines Road, MS126, La Jolla, CA 92037

[b]Department of Molecular Medicine, Scripps Research, 10550 North Torrey Pines Road, MB-102A, La Jolla, CA 92037

Abstract

Mimicking the ultrastructural morphology of the meniscus with nanofiber scaffolds, coupled with controlled growth-factor delivery to the appropriate cells, can help engineer tissue with the potential to grow, mature, and regenerate after *in vivo* implantation. We electrospun nanofibers encapsulating platelet-derived growth factor (PDGF-BB), which is a potent mitogen and chemoattractant in a core of serum albumin contained within a shell of polylactic acid. We controlled the local PDGF-BB release by adding water-soluble polyethylene glycol to the polylactic acid shell to serve as a porogen. The novel core-shell nanofibers generated 3D scaffolds with an interconnected macroporous structure, with appropriate mechanical properties and with high cell compatibility. Incorporating PDGF-BB increased cell viability, proliferation, and infiltration, and upregulated key genes involved in meniscal extracellular matrix synthesis in human meniscal and synovial cells. Our results support proof of concept that these core-shell nanofibers can create a cell-favorable nanoenvironment and can serve as a system for sustained release of bioactive factors.

GRAPHICAL ABSTRACT

We electrospun core-shell nanofibers encapsulating platelet-derived growth factor (PDGF-bb) in a core of serum albumin contained within a shell of polylactic acid. Transmission electron microscopy revealed the core of serum albumin containing PDGF-bb. Incorporating PDGF-bb increased cell viability, proliferation, and migration. Core-shell nanofibers can create a cell-favorable nanoenvironment and serve as a model system for sustained release of bioactive factors.

[*]**Corresponding author:** Darryl D. D'Lima (MD, PhD), Shiley Center for Orthopaedic Research and Education at Scripps Clinic, 10666 North Torrey Pines Road, MS126, La Jolla, CA 92037, **Phone:** +1 (858) 554-7011, ddlima@scripps.edu.

Author Contributions

J.B., M.K.L., and D.D.D. designed the study and wrote the manuscript in close collaboration with the other authors. J.B. and E. L. conducted cell culture studies and conducted histology and qPCR analyses. J.B conducted and interpreted the SEM analysis. J.B. conducted the *ex vivo* repair model. All authors discussed the results and approved the final version of the article.

Disclosures: The authors have no conflicts of interest to declare.

Keywords

Co-axial electrospinning; Core-shell structure; Nanofibers; Tissue engineering; PDGF-BB; Meniscus

Background

Tissue engineering combines methods from material science engineering and life sciences to generate artificial constructs for regenerating new tissue. Dense connective tissue of the musculoskeletal system functions in challenging biomechanical environments. In order to resist repetitive mechanical loads, tissues such as the tendons and ligaments,[1] the knee meniscus,[2] and the annulus fibrous of the intervertebral disk,[3] consist of dense and highly aligned extracellular matrices (ECMs). Electrospinning is an attractive approach to engineer connective tissue such as the meniscus with structural, mechanical, and biochemical properties similar to native tissue.[4–6]

In addition to using the appropriate cells and scaffold materials, bioactive molecules such as growth factors that control cell proliferation, differentiation, migration, and ECM synthesis are critical to the success of a tissue-engineered construct. Supplying growth factors directly into the culture medium at regular intervals is only feasible *in vitro.* For *in vivo* applications, it is desirable to have a sustained release of growth factors from the scaffolds.

Biodegradable polymers have been used as reservoirs to modulate release kinetics of proteins and small molecules.[7] Poly(D, L lactide-co-glycolide) (PLGA) is a biodegradable polymer that is commonly formulated as microspheres, which degrades over time and releases the encapsulated bioactive molecules. However, the degradation lowers local pH, which can destabilize the acid-labile growth factors.[8] We have previously shown that polylactic acid (PLA) is an attractive polymer for electrospinning scaffolds that approaches the mechanical properties of the human meniscus and can be used to engineer meniscogenic tissues.[9]

PLA has a much slower degradation rate than PLGA and is therefore less likely to affect the local pH.[10–12] For example, the monomer content released from PLA has been reported to be ~14-fold less than PLGA 50/50 over a 4-week incubation in buffered media.[10] PLA has a wet-strength half-life of 6 months, which makes it useful for biodegradable meniscal repair devices.[13] Meniscal repair devices manufactured from PLA (e.g., Biostinger, meniscal screws, and meniscus arrows) preserve their initial strength even after six months.[14–16]

Blending nonspinnable molecules, such as growth factors, with electrospinnable polymers can compromise structural properties and can result in a burst release rather than a controlled release. Therefore, we elected to coaxially spin a core of bovine serum albumin (BSA) containing a growth factor in a shell of PLA. This approach to co-axial electrospinning falls into the same biophysical category as reservoir-type release, similar to PLGA spheres, but without the undesirable effect of low pH caused by rapid biodegradation of PLGA.[8] To control the release of growth factors contained in the core without increasing the rate of PLA

degradation, we used a water-soluble porogen. PEGs have been proposed to enhance protein release from slowly degrading PLA microspheres.[17]

Mimicking the ultrastructural morphology of the meniscus with nanofiber scaffolds, coupled with controlled growth-factor delivery to the appropriate cells, can engineer tissue that continues to grow, mature, and regenerate after *in vivo* implantation. For proof of concept, we used platelet-derived growth factor-bb (PDGF-BB), a powerful mitogen and chemoattractant that stimulates the proliferation and recruitment of cells.[18] PDGF is a locally produced mitogen for cells of mesenchymal origin such as progenitors, pericytes, fibroblasts, and chondrocytes.[19–21] Other important actions include angiogenesis, chemotaxis, and enhanced collagen synthesis.[22,23] Meniscal cells respond to PDGF with increased proliferation, collagen, and proteoglycan synthesis.[24]

Our primary hypothesis was that encapsulating PDGF-BB in the core would enhance cell proliferation and infiltration and would upregulate key genes involved in meniscal tissue synthesis. Our secondary hypothesis was that incorporating a porogen in the shell would enhance the local release of PDGF-BB. As proof of concept, we tested human synovial-derived cells as a potential source for tissue engineering and documented their performance relative to human meniscal cells.

Methods

Fabrication of core-shell scaffolds

A dual concentric nozzle (NNC-DN-1621, NanoNC, South Korea, Figure 1, A) was used for co-axial electrospinning to generate core-shell fibers with a core of BSA and a shell of PLA. BSA solution (1% w/v in phosphate buffered solution [PBS], Fisher, Pittsburgh, PA) or FITC- BSA (1% w/v in 10 mM Tris, Sigma-Aldrich, St. Louis, MO) was prepared with or without PDGF-BB (20 μg/ml, PeproTech, Rocky Hill, NJ). PLA solution (10% w/v, Mw = 100,000, NatureWorks, Minnetonka, MN) with 0, 1, 10, and 100 mg/ml polyethylene glycol (PEG) (Mw = 8,000, Sigma-Aldrich) was prepared by dissolving in 1,1,1,3,3,3-hexafluoro-2-propanol (HFIP, Chem-Impex International Inc., Wood Dale, IL). The PLA and BSA solutions were placed in different syringes, which were individually actuated by syringe pumps (KDS200, KD Scientific Inc., Holliston, MA) at a feed rate of 2 and 1 mL h^{-1}, respectively (Figure 1, B). The coaxial scaffolds were electrospun on a drum cylinder rotating at 2400 rpm to generate a predominantly parallel alignment.[5, 6] The applied voltage was adjusted between 15 and 20 kV using a voltage regulator DC power supply (NNC-30kV-2mA portable type, NanoNC) to induce a polymer jet. The scaffolds were stored at 4 °C before use.

Scaffold ultrastructure

Core-shell nanofibrous scaffolds were incubated in 1 ml of 1x PBS at 37 °C for the selected duration, were dried in a desiccator for one day, and were coated with iridium using a sputter coater (Emitech K575X, EM Technologies Ltd, Ashford, England) for scanning electron microscopy (SEM, Philips XL30, FEI Co., Hillsboro, OR) with an accelerating voltage of 10 kV. The core-shell structure of the co-axial electrospun nanofibers was examined via

transmission electron microscopy (TEM, FEI Tecnai 12 Spirit, FEI Co., Hillsboro, OR) with a voltage of 120 kV. The samples for TEM were prepared by directly depositing the as-spun nanofibers onto a copper grid on a flat plate as a collector. The samples were dried in a vacuum oven at room temperature for 48 h before TEM imaging. The diameters of the core and shell of the electrospun fibers were measured using image-processing software (Image J, National Institutes of Health, Bethesda, MD).

Scaffold mechanical testing

Tensile testing after hydration was performed as described previously.[5] Scaffolds were cut into dog-bone shaped specimens with a gauge length of 8 mm and gauge width of 2 mm using a custom aluminum die cutter. Each specimen was immersed in 1x PBS for 2 h at room temperature for hydration before testing. The thickness of each scaffold was measured using a digital caliper. Test specimens (N = 10 per group) were mounted in the grips of a uniaxial testing machine (Instron® Universal Testing Machine, 3342 Single Column Model; Norwood, MA) with a 500 N load cell and were tested to failure at a displacement rate of 1 mm sec^{-1}. The slope of the linear portion of the stress-strain curve was used to calculate the tensile modulus. The maximum load before failure was used to calculate the ultimate tensile strength (UTS).

Release kinetics of BSA and PDGF-BB

FITC-BSA was used to confirm the presence and distribution of BSA cores in the PLA/PEG nanofibers deposited on microscope glass slides, which were imaged on a laser confocal scanning microscope (LSCM, Zeiss LSM 710, Okerkochen, Germany). The excitation and emission wavelengths were 488 and 535 nm, respectively. Pure PLA fibers were used as negative control to adjust laser intensity and gain to remove background fluorescence from the PLA fiber sample.

To measure the effect of PEG on protein release kinetics, scaffolds (N = 4 each) electrospun with a core of BSA in shells of PLA containing 0, 1, 10, or 100 mg/ml PEG were incubated in 1 ml of 1x PBS at 37°C without shaking or stirring. The supernatant was then removed and was replenished with fresh PBS solution at predetermined time intervals up to 75 days. The BSA levels in the supernatant were measured using the micro-BCA™ protein assay.

Core-shell nanofibrous mats were electrospun with a shell of PLA solution (with or without PEG 1 mg/ml) and with a core of 1% BSA (with or without 20 μg/ml PDGF-BB). Electrospun scaffolds (N = 4) were incubated in 1 ml of 1x PBS at 37 °C, without shaking or stirring. The supernatant was then removed and replenished with fresh PBS solution at predetermined time intervals (up to 75 days). The released PDGF-BB was measured using an enzyme-linked immunosorbent assay (ELISA) that was performed according to the protocol provided by the manufacturer (R&D systems, Minneapolis, MN).

Tissue harvesting and cell isolation

With Scripps Institutional Review Board approval, normal human menisci and synovial tissues were obtained from six donors (mean age, 33 ± 8.07; age range, 17–35 years; 1 female and 5 males). The avascular region of the meniscus, which comprised the inner two

thirds of each meniscus and the synovial tissues were harvested, rinsed with sterilized 1x phosphate-buffered saline (1x PBS). After mincing with a surgical blade, the fragments were placed for overnight digestion under constant rotation at 37°C with collagenase (2 mg mL^{-1}; C5138, Sigma-Aldrich) in DMEM (Mediatech Inc., Manassas, VA) and 1% Penicillin-Streptomycin-Fungizone (Life Technologies, Carlsbad, CA). The digested tissues were filtered through 100 μm cell strainers (BD Biosciences, San Jose, CA) and the cells were seeded in high-density monolayer culture in DMEM (Mediatech) supplemented with 10% calf serum (Omega Scientific Inc. Tarzana, CA) and 1% Penicillin-Streptomycin-Glutamine (Life Technologies). The freshly isolated meniscus and synovial cells were cultured for three passages before seeding onto electrospun scaffolds.

Cell seeding

Human meniscal and synovial cells were seeded at a cell density of 0.5×10^6 per scaffold onto 10 mm diameter disks cut from the following types of electrospun scaffolds: (1) BSA core in PLA shell, (2) BSA + PDGF-BB core in PLA shell, (3) BSA core in PLA+PEG shell and, (4) BSA + PDGF-BB core in PLA+PEG shell. The PLA/PEG shell contained 1 mg/ml PEG. Cell-seeded scaffolds were cultured in 6-well plates and were maintained in 3 mL of DMEM (Mediatech) supplemented with 10% calf serum (Omega Scientific Inc.) and with 1% Penicillin- Streptomycin-Glutamine (Life Technologies) for 1 day for initial cell attachment and scaffold colonization. The culture medium was then changed to serum-free ITS+ medium (Sigma- Aldrich) that was supplemented with subsequent medium changes every 3 to 4 days for 2 weeks.

Cell viability

The viability of cells on the scaffolds cultured for 2 weeks was measured using Calcein-AM and Ethidium Homodimer-1 (Live/Dead kit, Life Technologies) following the manufacturer's protocol. Cells were imaged using a laser confocal scanning microscope (LSCM, Zeiss LSM 710). For quantitative analysis, the fluorescence intensity of the live cells (green) and dead cells (red) was calculated with Image Pro Premier software (9.2, Media Cybernetics Inc., Rockville, MD).

Gene expression

Total RNA was isolated using the RNeasy Mini Kit (Qiagen, Hilden, Germany) and first strand cDNA was made as per manufacturer's protocol (Applied Biosystems, Foster City, CA). Quantitative RT-PCR was performed using TaqMan® gene expression reagents. COL1A1, ACAN, SOX9, COMP, THY-1, CHAD, PDGFRβ, CSPG4, ACTA2, VEGFA and GAPDH were detected using Assays-on-Demand™ primer/probe sets (Applied Biosystems). Expression levels were normalized to GAPDH using the recommended the ΔCt method and fold change was calculated using the $2^{-\Delta\Delta CT}$ formula.

Histology, and immunohistochemistry (IHC)

After 2 weeks in culture, scaffolds were fixed in Z-Fix (ANATECH, Battle Creek, MI) for 2 days and were embedded in paraffin. Sections (5–7 μm thick) were stained with hematoxylin and eosin (H&E) for morphological analysis and with Safranin O Fast Green to assess

glycosaminoglycan distribution. For detection of PDGFRβ by immunohistochemistry, cut sections were treated with hyaluronidase for 2 h and were incubated overnight at 4 °C with a primary antibody against PDGFRβ (ab107169, 1:200 dilution, Abcam, Cambridge, MA). ImmPRESS-HRP anti-rabbit IgG (MP-7401, Vector Laboratories, Burlingame, CA) was used as a secondary antibody for 30 min. An isotype control was used to monitor nonspecific staining. To count cells, sections were stained with VECTASHIELD® mounting medium containing 4′,6-diamidino-2-phenylindole (DAPI) (Vector Laboratories).

Statistical analysis

Kruskal-Wallis and Mann-Whitney tests were used to detect statistically significant differences in fiber diameter, mechanical properties, and gene expression between scaffold and cell types. *P* values less than 0.05 were considered statistically significant.

Results

Ultrastructure of core-shell fibers

SEM (Figure 1, C) highlights the extensive surface area of the core-shell fibrous scaffolds and the interconnected porous architecture. TEM images (Figure 1, D) revealed the core-shell structure of individual fibers consisting of a lighter shell of PLA containing a darker core of BSA. The presence of clear boundaries between the BSA core and the PLA shell indicated that the two fluids did not mix significantly during electrospinning. The average thickness of the BSA core increased with PEG concentration: 24.17 ± 4.54 nm, 29.66 ± 5.51 nm, 37.04 ± 4.64 nm, and 45.79 ± 4.88 nm at PEG concentrations of 0, 1, 10, 100 mg/ml, respectively, Figure 1, E.

PEG concentration affects structural properties of PLA

The mechanical properties of core-shell nanofibers are important for successful applications in meniscal tissue engineering. PEG is water-soluble and acts as a porogen; however, PEG may reduce the structural strength of PLA. We therefore tested the effect of PEG on mechanical properties of the core-shell electrospun scaffolds at four different concentrations of PEG (0, 1, 10, and 100 mg/ml, Figures 1, F and G). The tensile modulus for the scaffolds electrospun with concentrations of PEG at 10 and 100 mg/ml was significantly greater than scaffolds electrospun with concentrations of PEG at 0 and 1 mg/ml. These differences were also reflected in the tensile strength of scaffolds with PEG at 10 mg/ml and 100 mg/ml, which generated a significantly higher tensile strength than PEG at 0 and 1 mg/ml.

Increasing PEG concentration increased the average fiber diameter of core-shell scaffolds (SEM, Figure 2). However, this increase in fiber diameter reduced over time in culture (up to 40 days in 1 ml of 1x PBS at 37 °C) which was consistent with the expected loss of PEG over time.

Laser confocal scanning microscopy of scaffolds spun with cores of fluorescent-labeled BSA in PLA shells confirmed the encapsulation of BSA inside the nanofibers (Figure 3, A). The fluorescent signal increased with the concentration of PEG that corresponded with the increased fiber diameter.

PDGF-BB release from BSA core

We measured PDGF-BB release from PDGF-BB in PLA or PLA with 1 mg/mL PEG nanofibers. Less than 10% of the encapsulated growth factor was released from the core-shell nanofibers without PEG in the shell. Adding 1 mg/ml PEG to the PLA increased PDGF-BB release to almost 100% in 75 days (Figure 3, B). We therefore decided to electrospin fibers with PDGF-BB and PLA containing 1 mg/ml PEG scaffolds for cellular experiments.

Cell seeding and viability

Human meniscal avascular and synovial cells were cultured on electrospun mats with or without PDGF-BB, and with or without 1 mg/ml PEG. Cell attachment, morphology, and alignment are depicted in representative confocal images in Figure 4, A, which provided evidence of high cell viability in the scaffolds. In general, the overall viability of synovial cells was equivalent to that of meniscal cells (Figure 4). On quantitative analysis (Figures 4, B and 4, C), the presence of PDGF-BB increased the viability of meniscal and synovial cells (n = 3 donors, 3 replicates). There was an insignificant increase in the fluorescent intensity (<1 unit) of dead meniscal cells on scaffolds with PDGF-BB relative to that of dead meniscal cells without PDGF-BB.

PDGF-BB effects on gene expression.

Human meniscal and synovial cells cultured on core-shell nanofibers expressed significantly higher levels of COL1A1, SOX9, COMP, PDGFRβ, CSPG4, and ACTA2 genes, and significantly lower levels of ACAN genes relative to monolayer-cultures (Figure 5). The synovial cells (but not the meniscal cells) expressed significantly higher levels of THY-1 and VEGFA genes relative to monolayer-cultured cells. In comparison to the meniscal cells, the synovial cells expressed significantly higher levels of SOX9, THY-1, PDGFRβ, CSPG4, ACTA2, and VEGFA. PDGF-BB induced significantly higher gene expression of COL1A1, SOX9, COMP, THY-1, PDGFRβ, CSPG4, and ACTA2. PEG had minimal effect on the tested genes.

PDGF-BB stimulates cell proliferation and infiltration

To assess the efficacy of PDGF-BB as a chemoattractant for meniscal and synovial cells, we measured the cell density and infiltration of both cell types into the electrospun mats as a function of PDGF-BB dose (Figures 6, A and 7, A). After 2 weeks of culture, the meniscal and synovial cells had infiltrated into electrospun mats that contained a core of PDGF-BB, by H&E, Safranin O Fast Green, and DAPI (Figures 6 and 7). In contrast, without PDGF-BB both cells types were predominantly restricted to the surface of the scaffolds. On immunohistochemistry, significantly greater PDGFRβ expression was noted in cells cultured on electrospun mats that contained a core of PDGF-BB.

The quantification of cell density on DAPI stained sections (Figures 6, B and 7, B) revealed that PDGF-BB encapsulated core-shell fibers generated significantly higher cell density for both cell types. In the absence of PDGF-BB, the cell density of synovial cells was higher than that of meniscal cells.

Discussion

Nanotechnology, such as electrospinning, provides opportunities to characterize, manipulate, and organize matter at the nanometer scale for tissue engineering. One of the challenges in electrospun tissue engineering is how to enhance cell proliferation and how to induce cell migration into the 3-dimensional scaffolds to support tissue neogenesis and function. This study presents a novel approach to leverage electrospinning to generate tissue-engineered scaffolds capable of a controlled growth factor delivery. As proof of concept for potential clinical translation, we studied the effect of the potent mitogen and chemoattractant (PDGF-BB) to present biochemical signals to cells for tissue engineering applications. The controlled local release of PDGF-BB induced distribution of human avascular meniscal cells and synovial cells throughout the scaffold resulting in effective synthesis of meniscal-like neotissue.

As proof of concept, Zhang *et al.,*[25] controlled the release of BSA from co-axial electrospun nanofibers with a core of BSA and a shell of poly(ϵ-caprolactone) (PCL). In that study, PEG was added to BSA to increase viscosity and to stabilize the BSA during electrospinning. In our experiments, we added PEG to the PLA sheath and showed that the release of BSA can be controlled by modulating the concentration of PEG in the PLA Adding PEG to PLA can increase the degradation rates of PLA. However, Zhang *et al* reported only a 4% loss in mass over 60 days after adding 10mg/mL of PEG to PLA.[26] In our study, adding PEG to PLA initially increased the overall diameter of core-shell nanofibers. PEG at a concentration of 1mg/mL did not affect the mechanical properties of the electrospun mats. Higher concentrations of PEG (up to 100mg/mL) increased the fiber diameter as well as the tensile stiffness; however, the fiber diameter decreased over 40 days of culture, presumably due to the loss of water-soluble PEG.

Only 10% of the PDGF-BB incorporated in the core was released after 75 days in culture when the PLA shell did not contain any PEG. To enhance the release of PDGF-BB, we added PEG to the PLA shell. Low molecular weight PEGs, which are water-soluble, function effectively as a porogen, are noncytotoxic and are filtered by the kidneys.[27, 28] By inducing pores in the PLA shell, one can modulate the release of proteins in the core without significantly increasing the rate of PLA biodegradation, thus preventing an undesirable lowering of the local pH.[8, 17] The critical period for meniscus repair is 6-12 weeks.[29] Adding just 1 mg/ml PEG to the PLA increased PDGF-BB release to over 80% in 6 weeks, and almost 100% in 75 days (Figure 3, B). This finding led us to conduct subsequent experiments with cells at 1 mg/ml of PEG in PLA core-shell fibers.

Heparin conjugation has been used to control the release of PDGF-BB from electrospun scaffolds to stimulate smooth muscle cells.[30, 31] That process, however, required multiple steps after electrospinning: cross-linking of gelatin, followed by conjugation of heparin, and then reacting with PDGF-BB before seeding cells. While PDFG-bb release was effectively controlled by heparin conjugation, cell infiltration was negligible within scaffolds consisting of fibers of 1μm diameter; fibers 3μm in diameter induced a modest increase in cell infiltration. Our technique involved one-step co-axial electrospinning before cell seeding and we achieved over 10-fold increase in cell proliferation and infiltration in scaffolds with

average fiber diameters of less than 1 μm. Despite obvious differences in the scaffold materials (PCL/gelatin versus PLA) and cell types (smooth muscle cells versus meniscal and synovial cells), we believe that the continued release of PDGF-BB from the fiber core accelerated cell infiltration, while heparin conjugation tended to bind PDGF-BB locally and limited its release.

Functionalizing the core-shell nanofibrous scaffolds with PDGF-BB enhanced the meniscogenic response in cells reflected by increased gene expression (COLA1, SOX9, ACAN, COMP, PDGFRβ, CSPG4, and ACTA2) relative to non-PDGF encapsulated core-shell scaffolds. COLA1, SOX9, ACAN, and COMP are important for the synthesis of fibrocartilage, which was reflected in the histological findings. PDGFRβ, CSPG4, and ACTA2 are markers for pericytes.[32] The upregulation of PDGFRβ was validated by IHC of the neotissue for PDGFRβ (the primary receptor for PDGF-BB). PDGFRβ stimulated cell growth, proliferation, differentiation, and extracellular matrix production.[18,33] Our findings of the beneficial effects of PDGF-BB are likely mediated in part via upregulation of PDGFRβ.

Several cell sources have been proposed for meniscus repair including meniscus fibrochondrocytes, chondrocytes, or bone marrow-derived mesenchymal stem cells. However, the ideal cell type for meniscus repair has not yet been established. We studied two different cell sources, human meniscus cells and synovial cells. The meniscal cells served as positive control; however, meniscal cells are not easily available for clinical applications. Synovial tissue can serve as a reservoir for stem cells that mobilize following trauma and that migrate to the injury site where, in cooperation with local cells, they participate in the repair response. Synovial cells can be harvested from synovium and can be readily expanded in culture.[34] Synovial cells have high chondrogenic potential;[35] intra-articular injections or implantation of aggregates of synovial cells promotes meniscus regeneration in rats, rabbits, pigs, and primates. ‘ ‘ The viability and proliferation of the synovial cells were at least equivalent to that of meniscal cells. In addition, expression of SOX9, THY-1, PDGFRβ, CSPG4, ACTA2, and VEGFA in synovial cells was significantly higher than that in the meniscal cells. These results support the potential for meniscal tissue engineering using synovial cells.

This study had the following limitations. Although we selected PDGF-BB as a proof of concept example of a growth factor with potential chemoattractant properties, we did not directly measure chemoattraction in this study. However, we have shown evidence of the efficacy of chemoattraction in previous studies involving heparin-bound PDGF.[4] *In vivo* experiments are planned to assess the clinical relevance of chemoattraction. We did not directly measure the bioactivity of released PDGF-BB. However, the positive effects on cell proliferation, distribution, and gene expression indicated that bioactivity during release was maintained. We only studied two human cell types (meniscal and synovial cells); it is possible that other cell sources will behave differently. We only studied the effects of one concentration of PEG on PDGF-BB release. Careful modulation of PEG concentration and of the electrospinning parameters may be required to generate the optimum rate of controlled release.

In summary, we fabricated a novel scaffold using nano fibers consisting of a shell of PLA containing a core of the potent growth factor PDGF-BB. PGDF-BB increased cell viability, proliferation, and distribution within the scaffold, and upregulated key genes involved in meniscal tissue synthesis. Integrating PEG as a porogen increased the local release of PDGF-BB. The performance of human synovial cells was at least equivalent to that of avascular meniscus cells, which supported their potential use for meniscal tissue engineering. These core-shell nanofibers can create a cell-favorable nanoenvironment and can serve as a model system for sustained release of bioactive factors. *In vivo* experiments are underway to document the effect of PDGF-BB to enhance migration of host cells into implanted scaffolds.

Acknowledgements

We are grateful to Judy Blake for copyediting.

Funding: This work was supported by the National Institutes of Health [grant number P01 AG007996]; the Shaffer Family Foundation; and by Donald and Darlene Shiley.

References

1. Benjamin M, Ralphs JR. Fibrocartilage in tendons and ligaments — an adaptation to compressive load. J Anat 1998;193:481–94. [PubMed: 10029181]
2. Petersen W, Tillmann B. Collagenous fibril texture of the human knee joint menisci. Anat Embryol (Berl) 1998;197:317–24. 10.1007/s004290050141 [PubMed: 9565324]
3. Hickey DS, Hukins DW. Relation between the structure of the annulus fibrosus and the function and failure of the intervertebral disc. Spine (Phila Pa 1976) 1980;5:106–16. [PubMed: 6446156]
4. Lee KI, Olmer M, Baek J, D'Lima DD, Lotz MK. Platelet-derived growth factor-coated decellularized meniscus scaffold for integrative healing of meniscus tears. Acta Biomater 2018;76:126–34. 10.1016/j.actbio.2018.06.021 [PubMed: 29908335]
5. Baek J, Sovani S, Choi W, Jin S, Grogan SP, D'Lima DD. Meniscal Tissue Engineering Using Aligned Collagen Fibrous Scaffolds: Comparison of Different Human Cell Sources. Tissue Eng Part A 2018;24:81–93. 10.1089/ten.TEA.2016.0205 [PubMed: 28463545]
6. Baek J, Sovani S, Glembotski NE, Du J, Jin S, Grogan SP, et al. Repair of Avascular Meniscus Tears with Electrospun Collagen Scaffolds Seeded with Human Cells. Tissue Eng Part A 2016;22:436–48. 10.1089/ten.TEA.2015.0284 [PubMed: 26842062]
7. Schwendeman SP, Costantino HR, Gupta RK, Langer R. Peptide, Protein, and Vaccine Delivery from Implantable Polymeric Systems: In: Park K (ed). Controlled Drug Delivery: Challenges and Strategies, 1st ed. Washington DC: American Chemical Society; 1997, p. 229–67
8. Estey T, Kang J, Schwendeman SP, Carpenter JF. BSA degradation under acidic conditions: a model for protein instability during release from PLGA delivery systems. J Pharm Sci 2006;95:1626–39. 10.1002/jps.20625 [PubMed: 16729268]
9. Baek J, Chen X, Sovani S, Jin S, Grogan SP, D'Lima DD. Meniscus tissue engineering using a novel combination of electrospun scaffolds and human meniscus cells embedded within an extracellular matrix hydrogel. J Orthop Res 2015;33:572–83. 10.1002/jor.22802 [PubMed: 25640671]
10. Giunchedi P, Conti B, Scalia S, Conte U. In vitro degradation study of polyester microspheres by a new HPLC method for monomer release determination. J Control Release 1998;56:53–62. [PubMed: 9801429]
11. Magre EP, Sam AP, 1997 Hydrolytic degradation of PLAGA, calculation of rate constants from various types of in vitro degradation curves J Control Release, pp 318–19
12. Shenderova A, 2000 The Microclimate in poly(lactide-co-glycolide) microspheres and its effect on the stability of encapsulated substances, Ohio State University, Columbus, Ohio

13. Athanasiou KA, Agrawal CM, Barber FA, Burkhart SS. Orthopaedic applications for PLA-PGA biodegradable polymers. Arthroscopy 1998;14:726–37. [PubMed: 9788368]
14. Becker R, Schroder M, Starke C, Urbach D, Nebelung W. Biomechanical investigations of different meniscal repair implants in comparison with horizontal sutures on human meniscus. Arthroscopy 2001;17:439–44. 10.1053/jars.2001.19975 [PubMed: 11337709]
15. Asik M, Atalar AC. Failed resorption of bioabsorbable meniscus repair devices. Knee Surg Sports Traumatol Arthrosc 2002;10:300–4. 10.1007/s00167-002-0304-0 [PubMed: 12355305]
16. Arnoczky SP, Lavagnino M. Tensile fixation strengths of absorbable meniscal repair devices as a function of hydrolysis time. An in vitro experimental study. Am J Sports Med 2001;29:118–23. 10.1177/03635465010290020201 [PubMed: 11292034]
17. Jiang W, Schwendeman SP. Stabilization and controlled release of bovine serum albumin encapsulated in poly(D, L-lactide) and poly(ethylene glycol) microsphere blends. Pharm Res 2001;18:878–85. 10.1023/A:1011009117586 [PubMed: 11474795]
18. Andrae J, Gallini R, Betsholtz C. Role of platelet-derived growth factors in physiology and medicine. Genes Dev 2008;22:1276–312. 10.1101/gad.1653708 [PubMed: 18483217]
19. Hammes HP, Lin J, Renner O, Shani M, Lundqvist A, Betsholtz C, et al. Pericytes and the pathogenesis of diabetic retinopathy. Diabetes 2002;51:3107–12. 10.2337/diabetes.51.10.3107 [PubMed: 12351455]
20. Betsholtz C Role of platelet-derived growth factors in mouse development. Int J Dev Biol 1995;39:817–25. [PubMed: 8645566]
21. Nimni ME. Polypeptide growth factors: targeted delivery systems. Biomaterials 1997;18:1201–25. 10.1016/S0142-9612(97)00050-1 [PubMed: 9300556]
22. Phillips GD, Marika Stone A. PDGF-BB induced chemotaxis is impaired in aged capillary endothelial cells. Mech Ageing Dev 1994;73:189–96. 10.1016/0047-6374(94)90051-5 [PubMed: 8057689]
23. Risau W, Drexler H, Mironov V, Smits A, Siegbahn A, Funa K, et al. Platelet-Derived Growth Factor is Angiogenic In Vivo. Growth Factors 1992;7:261–66. 10.3109/08977199209046408 [PubMed: 1284870]
24. Bhargava MM, Attia ET, Murrell GA, Dolan MM, Warren RF, Hannafin JA. The effect of cytokines on the proliferation and migration of bovine meniscal cells. Am J Sports Med 1999;27:636–43. 10.1177/03635465990270051601 [PubMed: 10496583]
25. Zhang YZ, Wang X, Feng Y, Li J, Lim CT, Ramakrishna S. Coaxial electrospinning of (fluorescein isothiocyanate-conjugated bovine serum albumin)-encapsulated poly(epsilon-caprolactone) nanofibers for sustained release. Biomacromolecules 2006;7:1049–57. 10.1021/bm050743i [PubMed: 16602720]
26. Zhang P, He Y- Y, Gao D, Cai Y, Liu B. Hydrolytic and thermal degradation of polyethylene glycol compatibilized poly(lactic acid)-nanocrystalline cellulose bionanocomposites. Appl Polym Sci 2019;136:46933.
27. Kim HK, Chung HJ, Park TG. Biodegradable polymeric microspheres with “open/closed” pores for sustained release of human growth hormone. J Control Release 2006;112:167–74. 10.1016/j.jconrel.2006.02.004 [PubMed: 16542746]
28. Hedberg EL, Tang A, Crowther RS, Carney DH, Mikos AG. Controlled release of an osteogenic peptide from injectable biodegradable polymeric composites. J Control Release 2002;84:137–50. 10.1016/S0168-3659(02)00261-4 [PubMed: 12468217]
29. Barber FA. Meniscus repair aftercare. Sports Med Arthrosc 1999;7:43–47.
30. Qu D, Zhu JP, Lu HH. Controlled Release of TGF-β3 from Nanofiber Scaffolds Induces Fibrochondrogenic Differentiation of Stem Cells. Trans 63rd Orthop Res Society 2017;42:0279.
31. Lee J, Yoo JJ, Atala A, Lee SJ. The effect of controlled release of PDGF-BB from heparin-conjugated electrospun PCL/gelatin scaffolds on cellular bioactivity and infiltration. Biomaterials 2012;33:6709–20. 10.1016/j.biomaterials.2012.06.017 [PubMed: 22770570]
32. Olson LE, Soriano P. PDGFRbeta signaling regulates mural cell plasticity and inhibits fat development. Dev Cell 2011;20:815–26. 10.1016/j.devcel.2011.04.019 [PubMed: 21664579]

33. Wang H, Yin Y, Li W, Zhao X, Yu Y, Zhu J, et al. Over-expression of PDGFR-beta promotes PDGF-induced proliferation, migration, and angiogenesis of EPCs through PI3K/Akt signaling pathway. PLoS One 2012;7:e30503 10.1371/journal.pone.0030503 [PubMed: 22355314]

34. Kondo S, Muneta T, Nakagawa Y, Koga H, Watanabe T, Tsuji K, et al. Transplantation of autologous synovial mesenchymal stem cells promotes meniscus regeneration in aged primates. J Orthop Res 2017;35:1274–82. 10.1002/jor.23211 [PubMed: 26916126]

35. Sakaguchi Y, Sekiya I, Yagishita K, Muneta T. Comparison of human stem cells derived from various mesenchymal tissues: superiority of synovium as a cell source. Arthritis Rheum 2005;52:2521–9. 10.1002/art.21212 [PubMed: 16052568]

36. Katagiri H, Muneta T, Tsuji K, Horie M, Koga H, Ozeki N, et al. Transplantation of aggregates of synovial mesenchymal stem cells regenerates meniscus more effectively in a rat massive meniscal defect. Biochem Biophys Res Commun 2013;435:603–9. 10.1016/j.bbrc.2013.05.026 [PubMed: 23685144]

37. Nakagawa Y, Muneta T, Kondo S, Mizuno M, Takakuda K, Ichinose S, et al. Synovial mesenchymal stem cells promote healing after meniscal repair in microminipigs. Osteoarthritis Cartilage 2015;23:1007–17. 10.1016/j.joca.2015.02.008 [PubMed: 25683149]

38. Hatsushika D, Muneta T, Horie M, Koga H, Tsuji K, Sekiya I. Intraarticular injection of synovial stem cells promotes meniscal regeneration in a rabbit m model. J Orthop Res 2013;31:1354–9. 10.1002/jor.22370 [PubMed: 23595964]

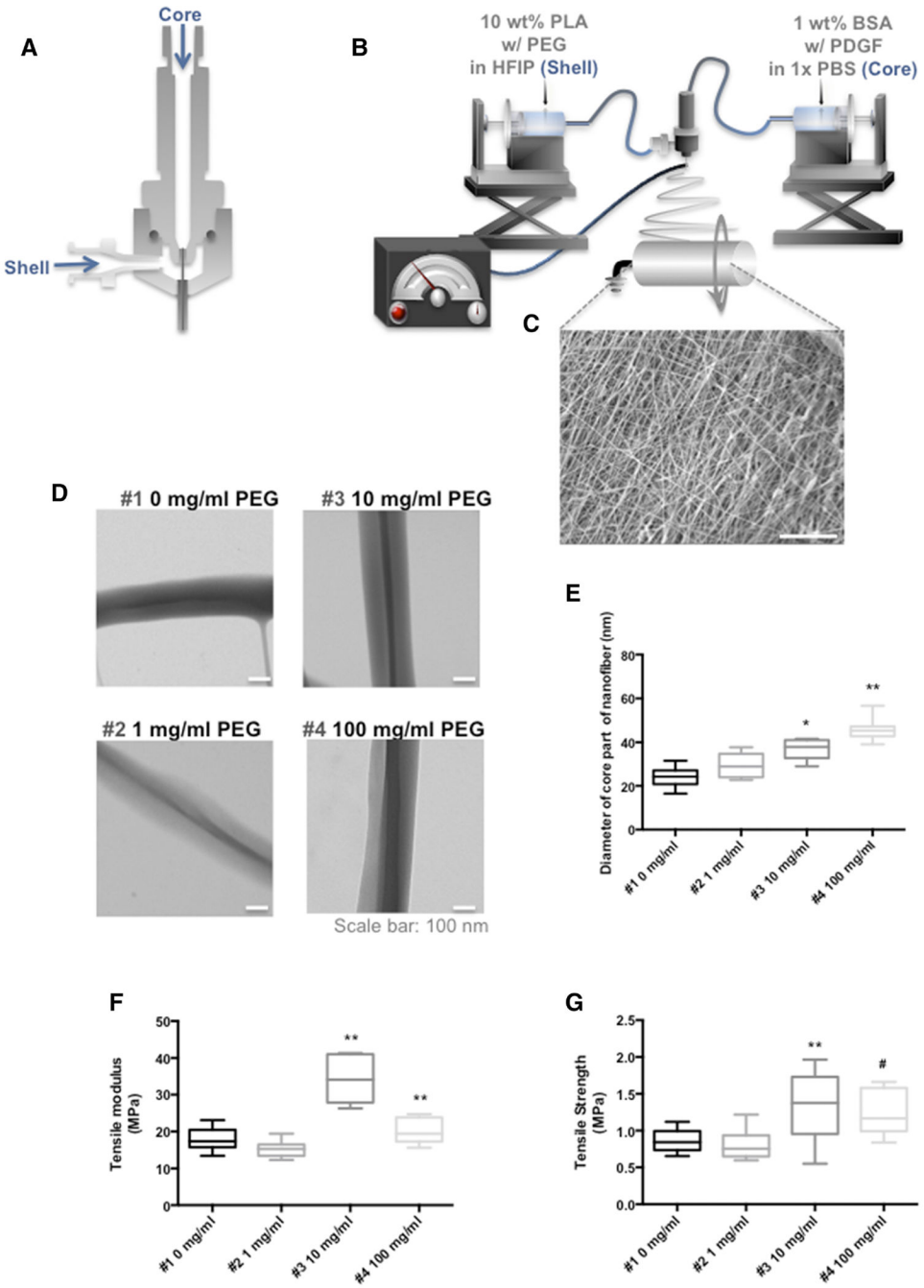

Figure 1. Co-axial electrospinning and structural properties of co-axial electrospun nanofibers.

(**A**) Schematic illustration of a co-axial electrospinning spinneret used to prepare core-shell nanofibers. (**B**) Overview of the core-shell electrospinning equipment. (**C**) SEM image of co-axial electrospun scaffold (Mag: 1250x; scale bar 20 μm). (**D**) Transmission electron microscopy images illustrating the presence of BSA cores in PLA shells with 0, 1, 10, and 100 mg/ml PEG (Mag: 30,000x; scale bar: 100 nm) (**E**) Average diameter of the BSA core increased with increasing concentrations of PEG. *= $P < 0.05$ compared to 0, and 1 mg/ml, **= $P < 0.05$ compared to 0, 1, 10 mg/ml (n = 10 per condition) (**F**) Tensile modulus and

(**G**) ultimate tensile strength of core-shell nano fibrous scaffolds with different concentration of PEG (0, 1, 10, and 100 mg/ml). **= $P < 0.05$ compared to 0, and 1 mg/ml, #= $P < 0.05$ compared to 10 mg/ml. (n = 10 per condition)

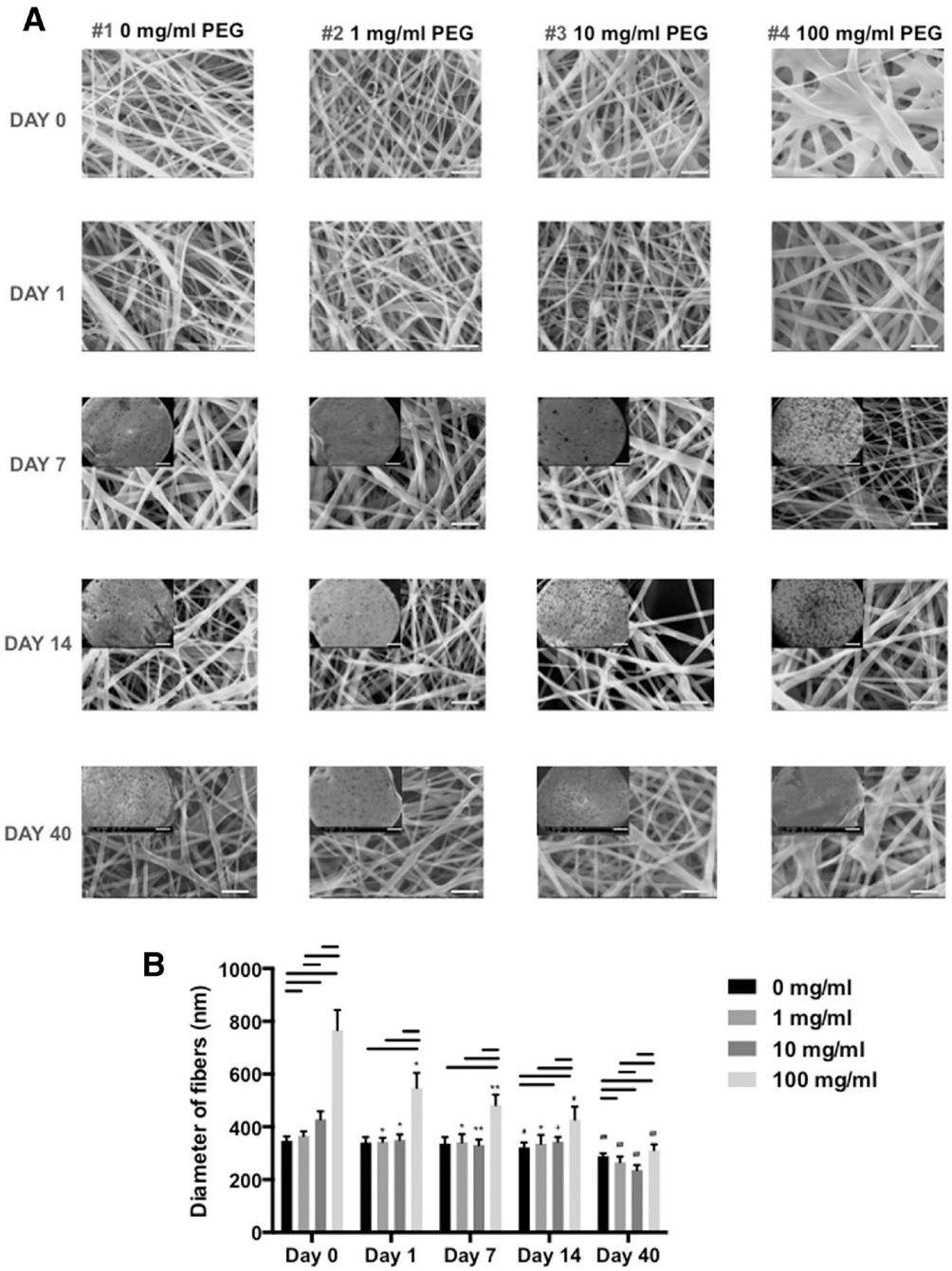

Figure 2. Size distribution of core-shell electrospun fibers with different PLA/PEG formulations over 40 days in phosphate buffered solution.

(**A**) SEM images of fibers (10% PLA + 0, 1, 10, or 100 mg/ml PEG) at day 0, 1, 7, 14, and 40 (Mag: 10,000x; scale bar: 5 μm). **Insert:** SEM images of each specimen (10% PLA + 0, 1, 10, or 100 mg/ml PEG) at day 7, 14, and 40 (Mag: 35x; scale bar: 500 μm) (**B**) Diameters of electrospun PLA nanofibers with different concentration of PEG cultivated in PBS over 40 days (electrospun fibers were examined by SEM and fiber size measured using ImageJ). Line= $P < 0.05$ between groups, *= $P < 0.05$ compared to 0 day, **= $P < 0.05$ compared to

0, and 1 day, #= $P < 0.05$ compared to 0, 1, and 7 day, ##= $P < 0.05$ compared to 0, 1, 7, and 14 day, += $P < 0.05$ compared to 0, and 7 day.

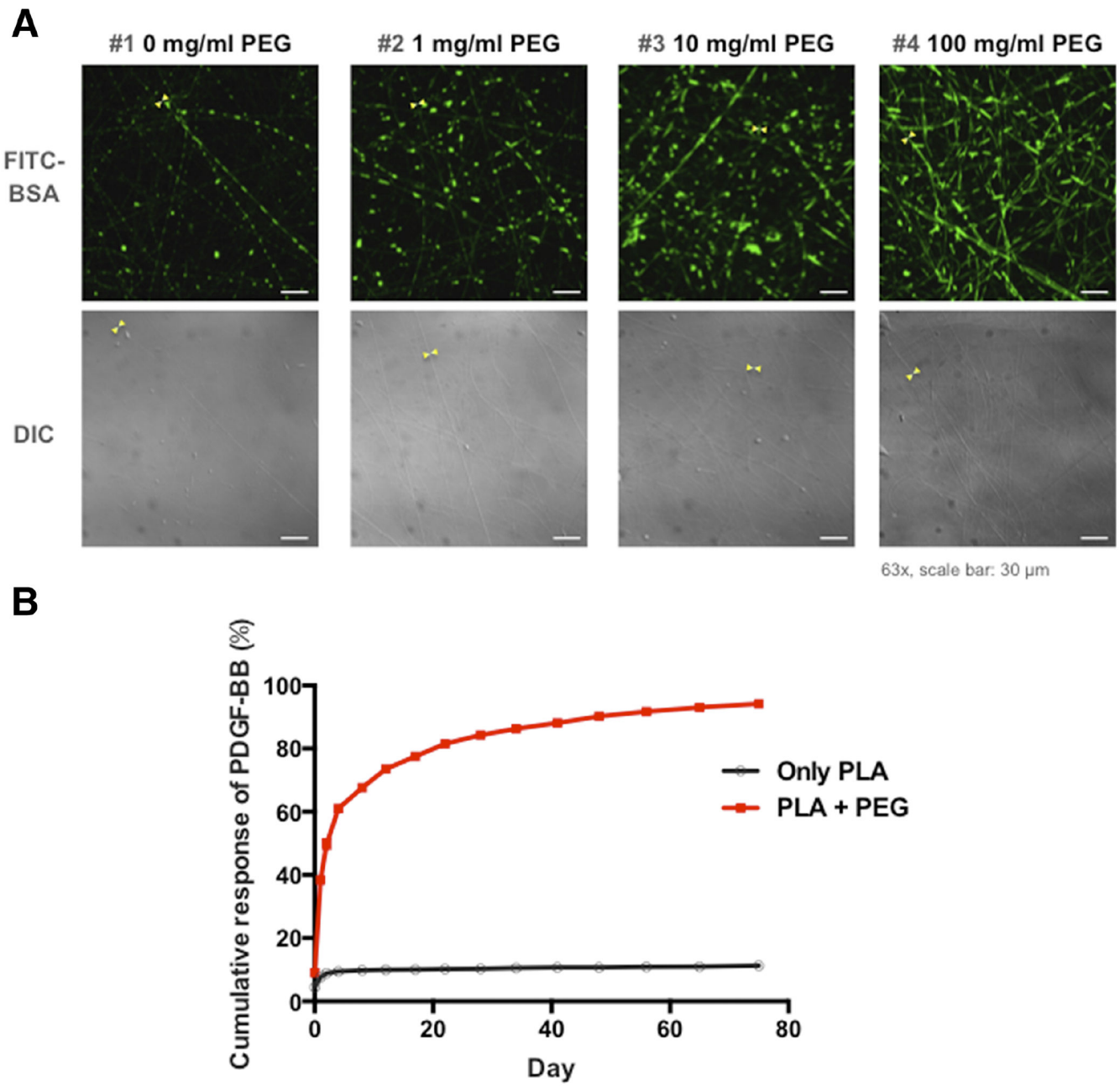

Figure 3. Encapsulation of FITC-BSA and PDGF-BB release from electrospun nanofibers.

(**A**) Laser confocal microscope and DIC images of core-shell nanofibers with FITC-BSA in formulations of PEG-blended PLA. (**B**) Controlled release of encapsulated PDGF-BB from PLA and PLA-PEG core-shell scaffolds. (10% PLA + 1 mg/ml PEG).

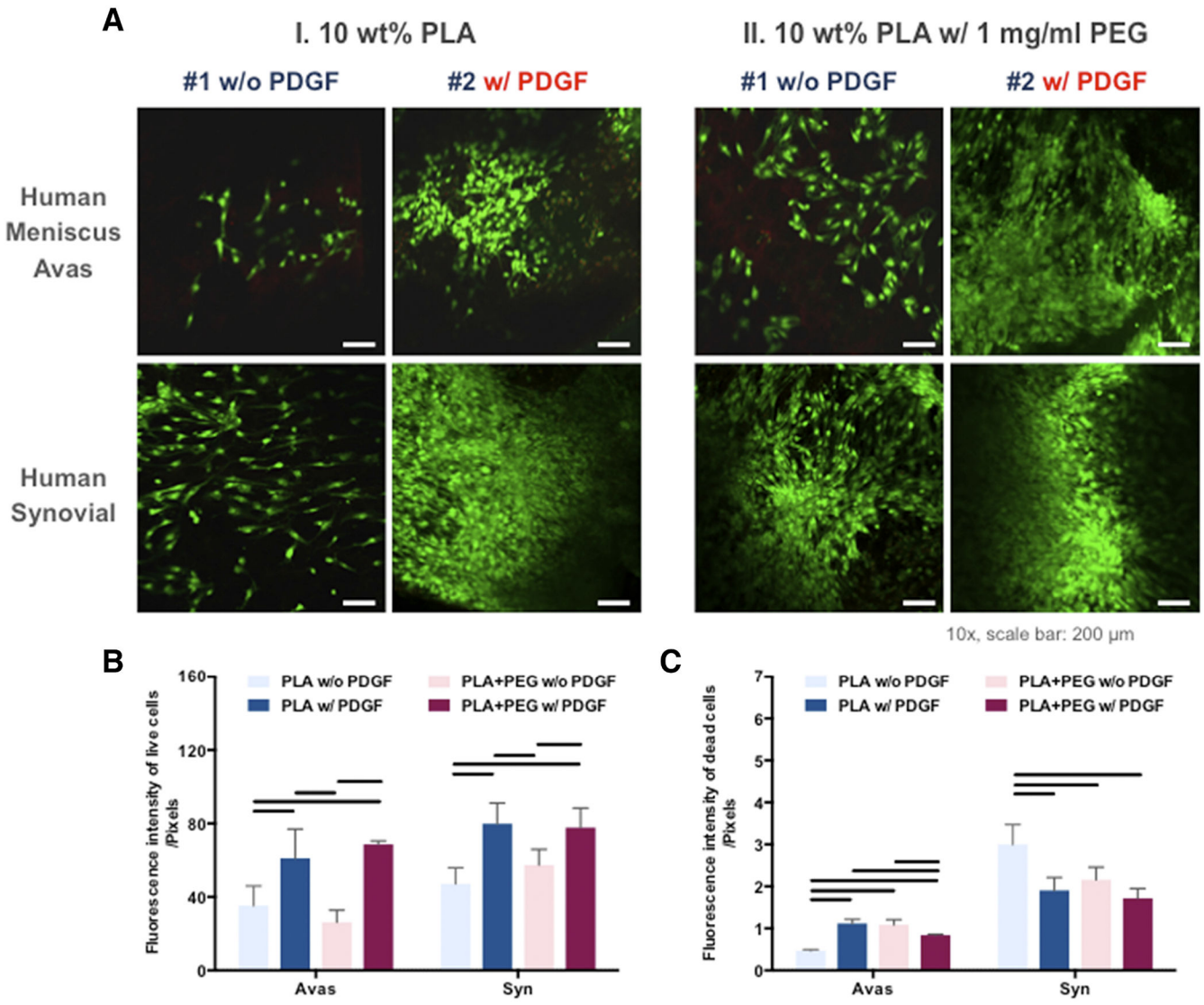

Figure 4. Cellular response of the human meniscus avascular and synovial cells cultured on PLA nanofibers with or without PDGF and with or without PEG.

(**A**) Confocal microscope images of human meniscus and synovial cells cultured on aligned PLA nanofibers demonstrating viability in confocal images (Mag. 10x; scale bar: 200 mm). (**B**) Quantitative analysis of fluorescent intensity of the live and dead meniscus and synovial cells in core-shell nanofibrous scaffolds (n = 3 donors, 3 replicates). Line= $P < 0.05$ between groups.

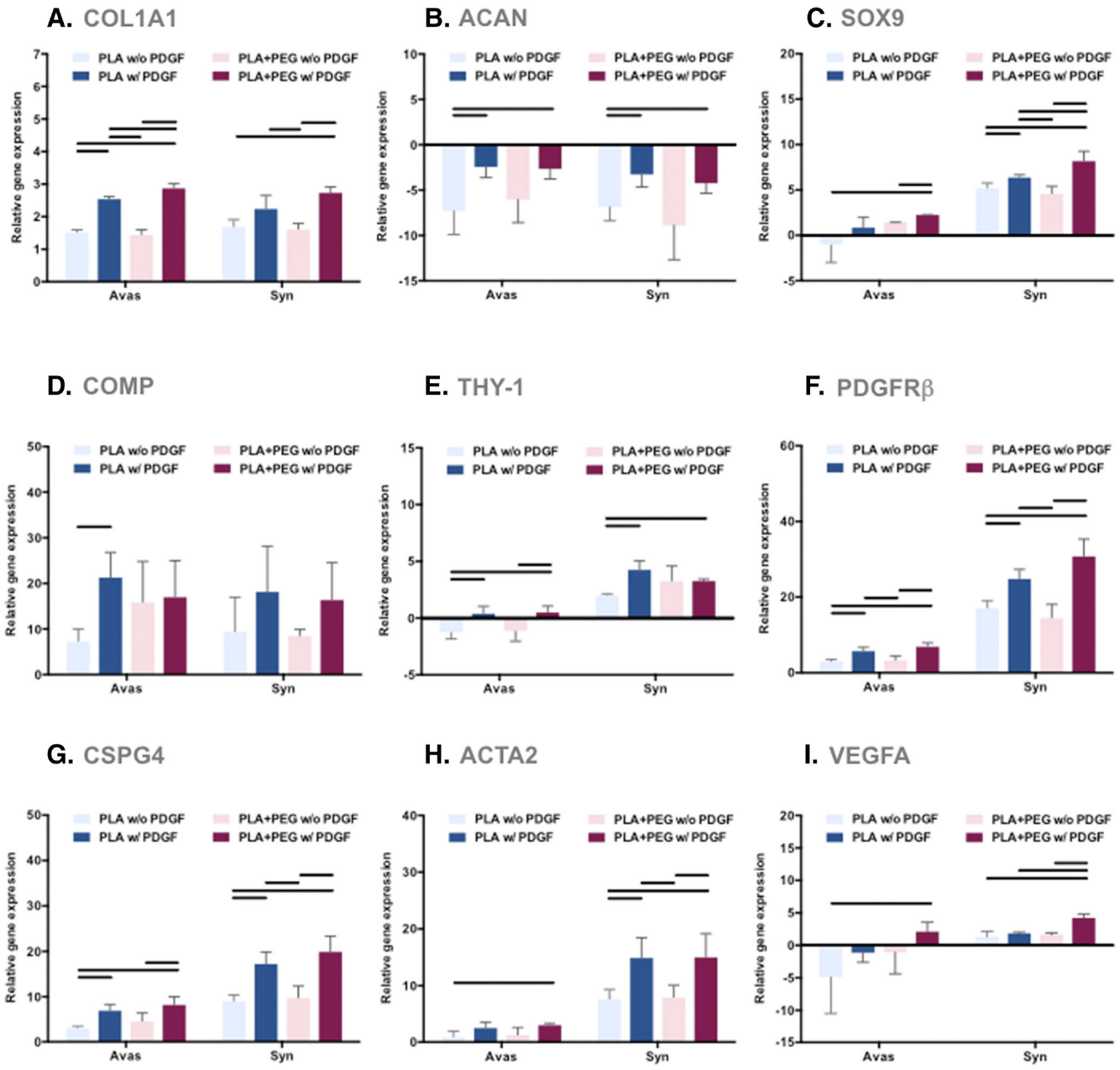

Figure 5. Gene expression levels of human meniscus avascular cells and synovial cells cultured on PLA scaffolds were compared to cells in monolayer culture.

Shown here are differential effects of PDGF-BB and PEG (3 donors, 3 replicates). (**A**) COL1A1 gene expression, (**B**) ACAN gene expression, (**C**) SOX9 gene expression, (**D**) COMP gene expression, (**E**) THY-1 gene expression, (**F**) PDGFRβ gene expression, (**G**) CSPG4 gene expression, (**H**) ACTA2 gene expression, and (**I**) VEGFA gene expression relative to monolayer controls. Line= $P < 0.05$ between groups.

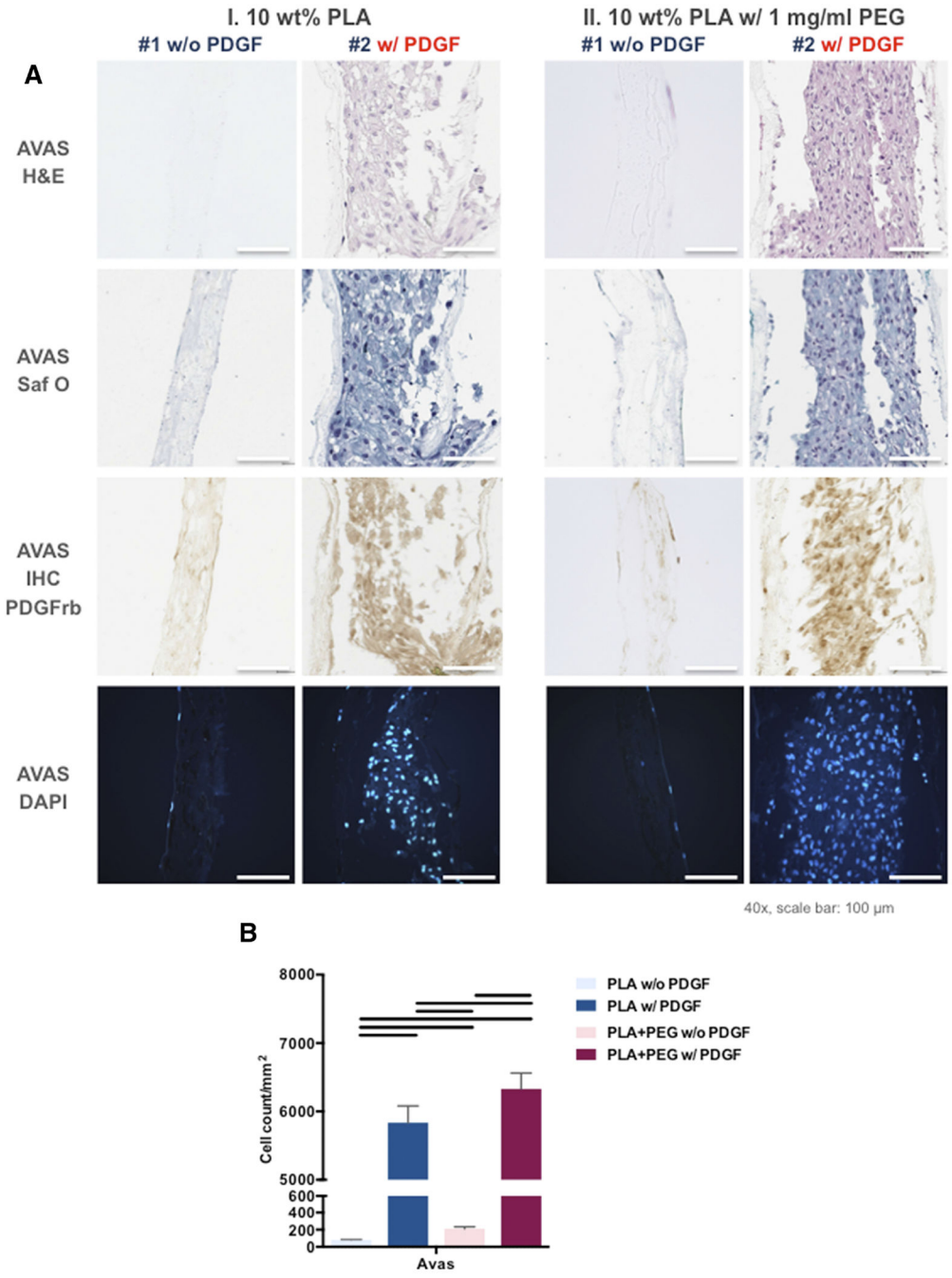

Figure 6. PDGF-BB significantly increased infiltration of human meniscus avascular cells into the scaffolds.

(**A**) Representative histologic images of core-shell nanofibers with human meniscus avascular cells: H&E, Safranin O Fast Green, DAPI, and PDGFRβ immunostaining (Mag.: 40x; scale bar: 100 μm). (**B**) Number of meniscus avas cells infiltrated into core-shell nanofibers (3 donors, 3 replicates). Line= $P < 0.05$ between groups.

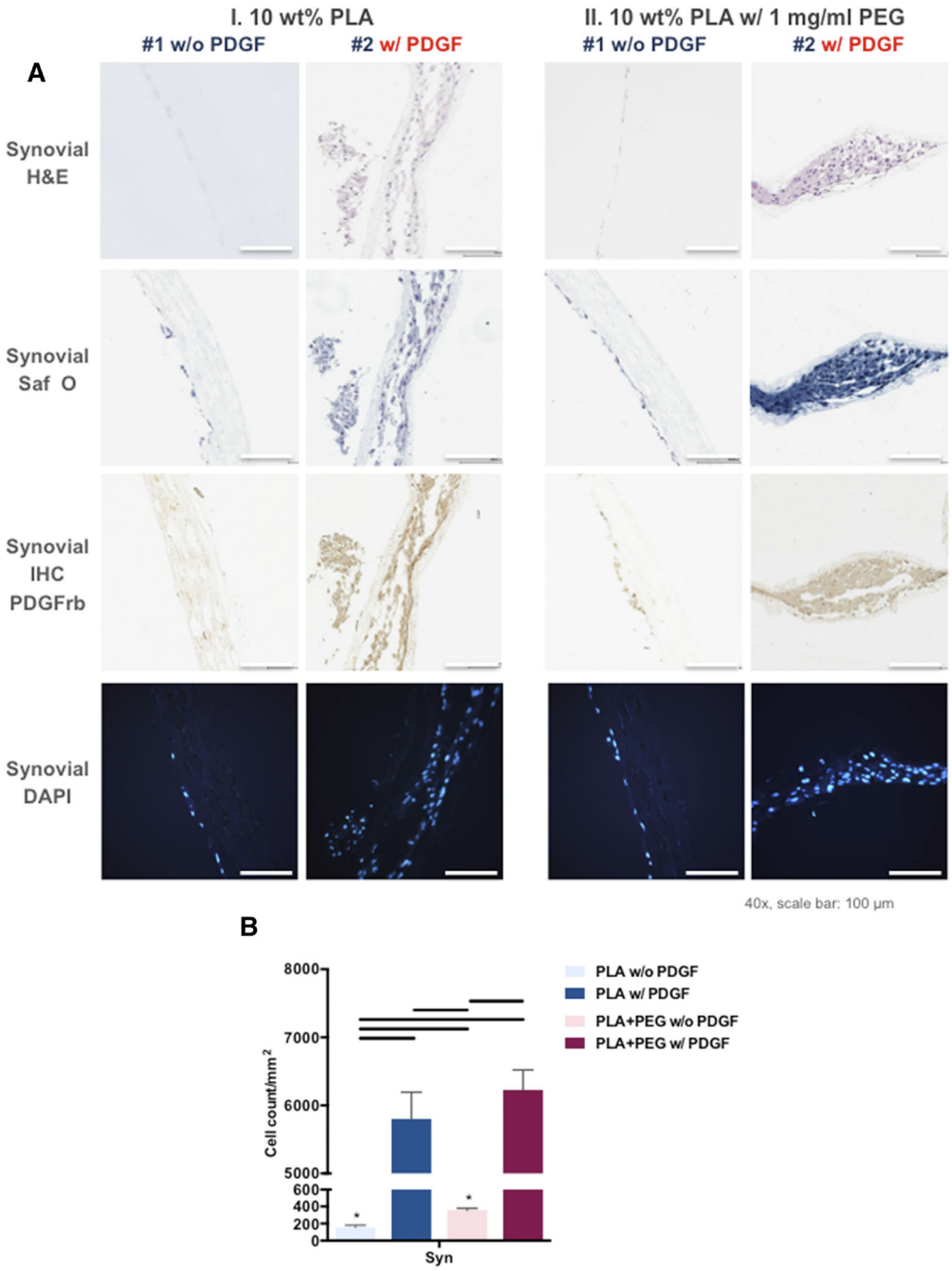

Figure 7. PDGF-BB significantly increased infiltration of human synovial cells into the scaffolds.

(**A**) Representative histologic images of core-shell nanofibers with human synovial cells: H&E, Safranin O Fast Green, DAPI, and PDGFRβ immunostaining (Mag.: 40x; scale bar: 100 μm). (**B**) Number of synovial cells infiltrated into core-shell nanofibers. Line= $P < 0.05$ between groups, *=$P < 0.05$ between each cell type.